Article

Discovery Medicine 2026; 38(206): 921–935
https://doi.org/10.24976/Discov.Med.202638206.75

CDDO-Me Attenuates Myocardial Injury in Coxsackievirus B3-Induced Viral Myocarditis by Suppressing the NLRP3-Related Inflammasome Through the NRF2/HO-1 Pathway

Chun Meng[1,*], Xiaoning Song[1], Xinran Cao[1], Runfa Zhou[1], Pengcheng Yan[1]

[1]Department of Cardiology, Shandong Provincial Hospital, Shandong University, 250021 Jinan, Shandong, China
*Correspondence: Carlmy7925@163.com (Chun Meng)
Submitted: 19 December 2025 Revised: 30 January 2026 Accepted: 25 February 2026 Published: 20 March 2026

Background: **Myocarditis is a rare, potentially fatal condition that particularly affects young people, with diverse causes ranging from viral infections (the most common in developed nations) to autoimmune diseases and toxins. Although acute viral myocarditis (VMC) is frequently subclinical and may resolve spontaneously, persistent inflammation causes continual myocyte damage, leading to intractable heart failure or death. Treatment options for chronic myocarditis remain inadequate. The primary purpose of this study was to investigate whether C-28 methyl ester for 2-cyano-3,12-dioxoolean-1,9-dien-28-oic acid (CDDO-Me), a potent Nuclear factor erythroid 2-related factor 2 (Nrf2) activator, alleviates coxsackievirus B3 (CVB3)-induced myocardial injury in viral myocarditis, potentially through activating the Nrf2/heme oxygenase-1 (HO-1) signaling axis to exert anti-inflammatory and antioxidant effects.**

Methods: **Male BALB/c mice were subjected to CVB3 treatment to establish a CVB3-induced VMC mouse model, and body weight loss and survival were documented. Then, an enzyme-linked immunosorbent assay (ELISA) for measuring myocardial injury marker and inflammatory indicator contents in plasma was conducted. Echocardiography was done to detect the mouse cardiac function. To observe alterations in myocardial tissue morphology, hematoxylin-eosin (H&E) staining was conducted. Furthermore, nucleotide oligomerization domain-, leucine-rich repeat-, and pyrin domain-containing protein 3 (NLRP3), apoptotic-associated speck-like protein containing a CARD (ASC) and Caspase-1/Cleaved contents in VMC mice and H9C2 cells were measured through Western blotting (WB), immunofluorescence analysis, and quantitative real-time polymerase chain reaction (qRT-PCR). Nrf2, P-Nrf2, HO-1 and NAD(P)H quinone oxidoreductase 1 (NQO-1) levels were also examined through immunofluorescence, WB, and qRT-PCR in mice and H9C2 cells after treatment with CVB3. Moreover, for exploring how Nrf2 affected CVB3-treated VMC *in vitro*, Nrf2 was downregulated in H9C2 cells by small interfering RNA (siRNA) transfection.**

Results: ***In vivo*** **experiments revealed that bardoxolone methyl (CDDO-Me) intervention significantly improved survival, body weight loss, myocardial injury, inflammatory reactions and ventricular systolic dysfunction in CVB3-induced VMC ($p < 0.05$, $p < 0.01$, or $p < 0.001$ vs. CVB3 group, where applicable). Immunofluorescence, WB, and qRT-PCR analyses further revealed that the expression of inflammasome-associated proteins such as NLRP3, ASC and Caspase-1/Cleaved Caspase-1 was significantly increased in CVB3-induced VMC mice ($p < 0.001$), and this change was reversed by CDDO-Me intervention ($p < 0.01$ or $p < 0.001$). Notably, the downregulation of Nrf2/HO-1 pathway-related proteins in CVB3-induced VMC mice was reversed by CDDO-Me treatment ($p < 0.05$, $p < 0.01$, or $p < 0.001$). *In vitro*, we observed that CDDO-Me intervention ameliorated the CVB3-induced decrease in viability and inflammatory reactions in H9C2 cardiomyocytes ($p < 0.001$). Correspondingly, NLRP3, ASC and Caspase-1 were highly expressed in H9C2 cells co-incubated with CVB3 ($p < 0.001$), and this high expression could be reversed by CDDO-Me intervention ($p < 0.05$, $p < 0.01$, or $p < 0.001$), suggesting that CDDO-Me intervention could reduce inflammation levels in H9C2 cells co-incubated with CVB3. Moreover, similar to the *in vivo* experimental results, our *in vitro* study suggested that the downregulating Nrf2/HO-1 pathway-related proteins in H9C2 cells co-incubated with CVB3 was also significantly reversed by CDDO-Me intervention ($p < 0.05$, $p < 0.01$, or $p < 0.001$). We then transfected H9C2 cells with Nrf2-specific siRNA to silence Nrf2, as Nrf2 knockdown significantly suppressed H9C2 cell survival and enhanced the inflammatory response ($p < 0.05$, $p < 0.005$, or $p < 0.001$).**

Conclusion: **CDDO-Me reduces myocardial injury and inflammatory reactions in CVB3-induced viral myocarditis, resulting from a reduction in the NLRP3 inflammasome induced by the regulation of Nrf2/HO-1.**

Keywords: bardoxolone methyl; viral myocarditis; Nrf2/HO-1 pathway; NLRP3; coxsackievirus B3

Introduction

Myocarditis results from different infectious pathogens, such as bacteria, fungi, viruses, protozoans, rickettsia, and chlamydia, alongside hypersensitivity and toxic responses [1–3]. Among them, viruses are usually reported in acute myocarditis. Viral myocarditis, a common myocardial inflammatory disease associated with viral infection, seriously endangers patients' quality of life. Coxsackievirus B3 (CVB3)-induced myocarditis is pathogenetically categorized into three stages: (1) acute viral replication, (2) autoimmune injury, and (3) cardiomyopathy progression (eventually developing into dilated cardiomyopathy (DCM)) [4]. CVB3 enters myocytes and causes a series of immune responses in infected individuals, although the induced myocarditis can be self-limiting [5]. When it enters acutely injured myocytes during autoimmune myocarditis for replication, it causes myocardial infarction, thereby triggering life-threatening adaptive immunity [6]. Persistent myocardial inflammation has been reported to lead to myocardial remodeling, which ultimately progresses to DCM or further deterioration of cardiac function, cardiac fibrosis, heart failure, or death [7]. At present, exact treatment strategies for viral myocarditis are lacking.

Nrf2 being an important antioxidant and anti-inflammatory factor *in vivo*, protects against various inflammatory disorders. Following activation, Nrf2 enters the nucleus, positively regulates HO-1 and executes anti-inflammatory functions through Nrf2/HO-1 pathway activation [8]. According to experimental results, the inflammatory factor NF-κB can be downregulated via Nrf2/HO-1 activation [9]. Besides, activating Nrf2/HO-1 pathway has been similarly shown to reduce NLRP3 content during osteoarticular inflammatory diseases and nervous system inflammatory diseases [10,11]. The NLRP3 inflammasome is a tightly regulated macromolecular protein complex that detects injury, initiates and amplifies inflammatory responses. It does so by activating caspase-1, cleaving pro-inflammatory cytokines such as pro-IL-1β and pro-IL-18 into their mature forms, and triggering inflammatory cell death. Inhibitors of the NLRP3 inflammasome, along with blockers of IL-1β and IL-18 activity have been shown to mitigate myocardial and pericardial injury, promote the resolution of inflammation, and help preserve cardiac function [12].

Bardoxolone methyl, as a C-28 methyl ester for 2-cyano-3,12-dioxoolean-1,9-dien-28-oic acid (CDDO) called CDDO-Me, serves as the artificial triterpenoid derivative and has been reported to possess more significant effects against tumor and inflammation [13]. CDDO-Me supplementation was also reported to promote Nrf2 expression in a prior study [14]. Therefore, this research investigated CDDO-Me for its function in reducing NLRP3 content in the myocardial tissue of mice with viral myocarditis via Nrf2/HO-1 pathway activation, thus reducing inflammatory injury.

Materials and Methods

Antibodies and Reagents

The rabbit anti-Nrf2 (16396-1-AP), anti-HO-1 (10701-1-AP) anti-NQO1 (11451-1-AP), anti-ASC (30641-1-AP) and anti-Caspase-1 (31020-1-AP) were from Proteintech (China); anti-NLRP3 (ET1610-93); goat anti-rabbit FITC-conjugated IgG (HA1004) were from HUABIO (China); rabbit anti-P-Nrf2 (#DF7519) were from Affinity (China); anti-β-actin (ab179467) were from Abcam (The USA); DAPI (C1005), goat anti-rabbit Cy3-conjugated IgG, H&E kit (C0105S) and CCK-8 (C0037) were from Beyotime (China), TRIzol Reagent (AM9738) and BCA protein assay kit (65453) were from Thermo Fisher, bardoxolone methyl (SMB00376, Sigma-Aldrich) and PVDF (HVLP09050, Merck Millipore) were used. The CK-MB (H197-1-1), cTnI (H149-2-1), TNF-α (H052-1-1), IL-6 (H007-1-1), IL-1β (H002-1-1) enzyme-linked immunosorbent assay (ELISA) kits were from Jian cheng Bio companies (Nanjing China). IL-18 (NBP2-76580) ELISA kits were from R&D systems; H9C2 cells (BNCC337726) were purchased from BNCC (Beijing, China), and had confirmed by the company's STR identification.

Animals and Treatments

The Institutional Animal Care and Use Committee of Shandong University approved our animal experiments (NO: 2022–302). We acquired 6–7-week-old male BALB/c mice maintained in specific pathogen-free environments, and allowed unrestricted access to food and water from the Institute of Medical Laboratory Animal Center, Shandong University (China). Following 1 week of adaptive feeding, the mice were randomized into four groups: (I) the control (n = 18), (II) CDDO-Me (n = 18), (III) CVB3 (n = 18) and (IV) CVB3+CDDO-Me (n = 18) groups. To establish a mouse model of viral myocarditis, the mice in CVB3 and CVB3+CDDO-Me groups were given a single intraperitoneal injection of CVB3 (1×10^5 plaque-forming units (PFU)) in PBS (100 µL), and the control and CDDO-Me mice were given identical PBS dosages [15]. After 24 h of CVB3 infection, the CDDO-Me and CVB3+CDDO-Me groups were intraperitoneally injected with CDDO-Me (5 mg/kg) [16] once daily for a 10-day period, and both CVB3 and control groups were given an intraperitoneal injection of an identical amount of saline. Mouse body weight and survival status were measured every day, with relevant curves documented on day 10, and echocardiography was performed on surviving mice. Finally, blood samples were collected and the hearts were removed from the thorax after euthanizing the mice by decapitation, and the hearts were then divided into two equal halves, with one portion soaked in 4% paraformaldehyde and the other frozen in liquid nitrogen before being stored at –80 °C for subsequent use.

Echocardiography

To assess cardiac structure and function in each of the mice treatment groups, we performed echocardiography using a high-resolution Vevo3100LT (Visual Ultrasonography, Toronto, Canada) imaging system. After anesthesia with 1.5% isoflurane, the mice left ventricles were recorded in M-mode at a papillary muscle level for measuring left ventricular end-diastolic diameter (LVEDD), left ventricular end-systolic diameter (LVESD), left ventricular anterior wall thickness (LVAWT), left ventricular ejection fraction (LVEF), as well as left ventricular fractional shortening (FS). Data from three measurements were averaged to obtain the final results.

Histopathology

Myocardial tissue was fixed within 4% paraformaldehyde at ambient temperature for a 24-h duration before paraffin embedding, sectioning in 5-µm sections, and hematoxylin and eosin (H&E) analysis, following specific protocols. After sealing, sections were visualized with a microscope (Nikon Tokyo, Japan), and the results were recorded.

The following morphological criteria were used to obtain a quantitative estimation of the histology: score 0, no damage; score 1 (mild), interstitial edema and focal necrosis; score 2 (moderate), diffuse myocardial cell swelling and necrosis; score 3 (severe), necrosis with presence of contraction bands and neutrophil infiltrate; score 4 (highly severe), widespread necrosis with presence of contraction bands, neutrophil infiltrate, and hemorrhage [17].

Biochemical Analysis

After 15 min of blood centrifugation (3000 r/min), the supernatant was harvested, and ELISA was employed for measuring creatine kinase isoenzyme (CK-MB), the cardiac isoform of troponin I (cTnI), interleukin-1beta (IL-1β), tumor necrosis factor-alpha (TNF-α), interleukin-6 (IL-6) and interleukin-18 (IL-18) contents in the serum, strictly following specific protocols (Jian Cheng, Nanjing, China). After collection, the cultured cell supernatants were subjected to an additional 20 min of centrifugation (1000 r/min) to remove cell debris and impurities, after which inflammation-related indicator (IL-1β, TNF-α, IL-6, IL-10) contents were determined *via* ELISA. The assay was carried out three times.

Cell Culture and Treatment

We cultivated H9C2 cells within Dulbecco's modified Eagle's medium (DMEM) (Gibco, NY, USA) containing 10% fetal bovine serum (FBS) alongside 1% penicillin/streptomycin under 37 °C and 5% CO_2 conditions. Nrf2-specific siRNA oligonucleotides (sense 5′-GGAGAGGGAAGAAUAAAGUTT-3′, antisense 5′-ACUUUAUUCUUCCCUCUCCTT-3′) were prepared by Genelily Biotech (Shanghai, China). Later, we utilized Lipofectamine 3000 transfection reagent for transfecting H9C2 cells transiently using si-Nrf2 or si-NC (Sense: 5′-CAGUAGUCUUGAGUCUAAT-3′, Antisense: 5′-UAUUAGACUCAAGAUACUG-3′).

Immunofluorescence (IF)

For immunofluorescence, fixed cells and myocardial tissue sections were subjected to overnight primary antibody incubation under 4 °C and additional 1 h of secondary antibody probing under 37 °C. Following 5 min of nuclear staining with DAPI, image acquisition was completed using the fluorescence microscope (Olympus, Japan).

Cell Viability Assay

We used the Cell Counting Kit-8 (CCK-8) assay kit for determining cell viability in accordance with specific protocols. H9C2 cells (0.5×10^4/well) were inoculated into 96-well plates before 12, 24 and 48 h of CDDO-Me treatment at various concentrations (0, 0.01, 0.05, 0.1, 0.5, or 1 µM), and the medium in each well was replaced with CCK-8 reagent (10 µL) contained within DMEM (90 µL) for another 1 h of incubation under 37 °C. Finally, absorbance was read at 450 nm (A450).

Western Blot Experiment

Protein isolation in both H9C2 cells and frozen heart tissues was completed. The cryopreserved heart tissues were ground as finely as possible using a mortar and liquid nitrogen, and an appropriate amount of tissue lysate was added according to the instructions. The samples were subsequently lysed on ice for 30 min and centrifuged, after which the supernatants were collected. The protein content of each sample was analyzed with a BCA kit to prepare a 2 µg/µL protein mixture. The protein extract was subsequently subjected to SDS-PAGE before transfer onto PVDF membranes. After 2 h of blocking using 5% bovine serum albumin under ambient temperature, the membranes underwent overnight primary antibody incubation (1:1000) under 4 °C and later another 1 h of horseradish peroxidase-labeled secondary antibody incubation (1:3000). The BioSpectrum Gel Imaging System (UVP, CA, USA) was subsequently utilized to detect protein bands. Gray values were also determined via ImageJ, and β-actin was the endogenous reference for normalization.

Quantitative Real-Time Polymerase Chain Reaction (qRT-PCR)

Myocardial tissue processing was implemented as described above, with total tissue and cellular RNA isolated with the TRIzol Reagent. Thereafter, RNA content was analyzed by NanoDrop ND-1000 spectrophotometer (Thermo Fisher Scientific, MA, USA). In addition, the first-strand cDNA synthesis kit (Applied Biosystems) was subsequently adopted for implementing com-

plementary DNA synthesis. The real-time PCR system (Roche,Basel, Switzerland) was utilized for the qRT-PCR, and the comparative CT ($\Delta\Delta$CT) approach was employed for calculating mRNA expression, with β-actin used for data normalization. **Supplementary Table 1** displays all primer sequences utilized.

Statistical Analysis

The data are presented as the means $\pm$ standard deviations (mean $\pm$ SD). Data analysis was completed with GraphPad Prism 10.6 (GraphPad, USA). Among-group differences were examined using one-way ANOVA with Tukey's post-hoc test. Alterations in body weight were detected by repeated-measures ANOVA. Kaplan–Meier (K–M) curves were plotted to test mouse survival status, whereas log-rank test was adopted for survival analysis. $p < 0.05$ suggested significant differences.

Results

CDDO-Me Improved Myocardial Damage, Inflammation, and Survival in Mice With Viral Myocarditis

Viral myocarditis, as previously described, is a severe condition associated with a high fatality rate and substantially threatens patient safety [1]. cTnI and CK-MB, markers of myocardial damage, were measured in the serum of mice to assess the degree of cardiac membrane integrity (Fig. 1A,B). Compared with control mice, CVB3 mice presented higher CK-MB and cTnI levels, whereas CDDO-Me markedly decreased their serum contents ($p < 0.001$). Additionally, the CVB3 group had apparently increased serum inflammatory cytokine contents, like TNF-α, IL-1β, IL-6 or IL-18; however, the CDDO-Me group showed remarkably decreased contents ($p < 0.001$) (Fig. 1C–F). The CVB3 group had a 50% survival rate at 10 days, which was markedly decreased relative to the 100% reported in the control and the CDDO-Me groups, while the value in CVB3+CDDO-Me group was 72.2%, which demonstrated an increase compared to the CVB3 group (Fig. 1G). Additionally, from Fig. 1H, both the CVB3 and the CVB3+CDDO-Me mice gradually decreased in body weight beginning on the third day of the experiment. The body weight of the CDDO-Me group slightly increased compared with the CVB3 group. Based on the above findings, an *in vivo* VMC model was successfully constructed; moreover, CDDO-Me treatment significantly improved myocardial injury and inflammation in CVB3-induced viral myocarditis.

CDDO-Me Inhibited Myocardial Remodeling

Myocardial structural changes and fibrosis occur in patients with viral myocarditis, especially during the immune activation phase. As shown in Fig. 2A, the heart size and shape of the mice in the control and the CDDO-Me injection groups alone were normal, and the surface was smooth; however, the hearts of mice from the CVB3 and the CDDO-Me+CVB3 groups were enlarged, the epicardial surface was not smooth, and excessive leukoplakia was observed, especially in the CVB3 group. Fig. 2B shows H&E-stained sections of the mice myocardium. Both the CDDO-Me and the control groups had normal myocardial cell sizes, uniform shapes, neatly arranged myocardial fibers, uniform and dense distributions, clear muscle fiber structures, and no obvious interstitial inflammatory cell infiltration. In contrast, the myocardial cell size and morphology differed between the CVB3 and the CVB3+CDDO-Me groups. They also had different degrees of myocardial cell edema, dissolution, and necrosis, while myofiber disarrangement, and vacuole-like changes, accompanied by the infiltration of excessive interstitial inflammatory cells, were observed in some myocardial cells. Blue inflammatory cell infiltration in the CVB3+CDDO-Me group was decreased relative to the CVB3 group, indicating that myocardial inflammation was inhibited. Fig. 2C–H show the statistical analysis results of cardiac ultrasound parameters. Relative to the control group, the LVAWT, LVEF, and FS markedly declined, whereas the systolic diameter apparently increased in the CVB3 group ($p < 0.001$), the above changes were remarkably alleviated in the CVB3+CDDO-Me group ($p < 0.001$, $p < 0.01$ or $p < 0.05$). Our study demonstrated that CDDO-Me attenuated myocardial remodeling caused by CVB3 infection in mice.

CDDO-Me Decreases NLRP3 Inflammasome-Related Protein Levels Within the Myocardium of Mice With CVB3-Mediated Viral Myocarditis

Viral myocarditis represents an inflammatory disease associated with viral infection and is characterized by inflammatory cell infiltration of the myocardium [16]. As shown in Fig. 3A,B, immunofluorescence revealed significantly increased inflammasome-related protein contents (NLRP3, ASC, Caspase-1) within the mouse myocardium after CVB3 infection ($p < 0.001$), and their contents decreased to varying degrees after CDDO-Me treatment ($p < 0.001$ or $p < 0.01$). As further confirmed by WB, NLRP3, Caspase-1, and ASC contents within mouse myocardium were notably increased in the CVB3 group ($p < 0.001$), whereas these changes were markedly suppressed after CDDO-Me treatment ($p < 0.001$) (Fig. 3C,D). As expected, NLRP3, Caspase-1, cleaved Caspase-1 and ASC protein-related mRNA levels were markedly elevated relative to control mice ($p < 0.001$), whereas CDDO-Me administration attenuated the CVB3-mediated upregulation of these mRNAs in VMC mice ($p < 0.001$ or $p < 0.01$) (Fig. 3E). Our findings revealed that CDDO-Me treatment decreased NLRP3 inflammasome activation in the myocardial tissue of mice with myocarditis resulting from CVB3 infection.

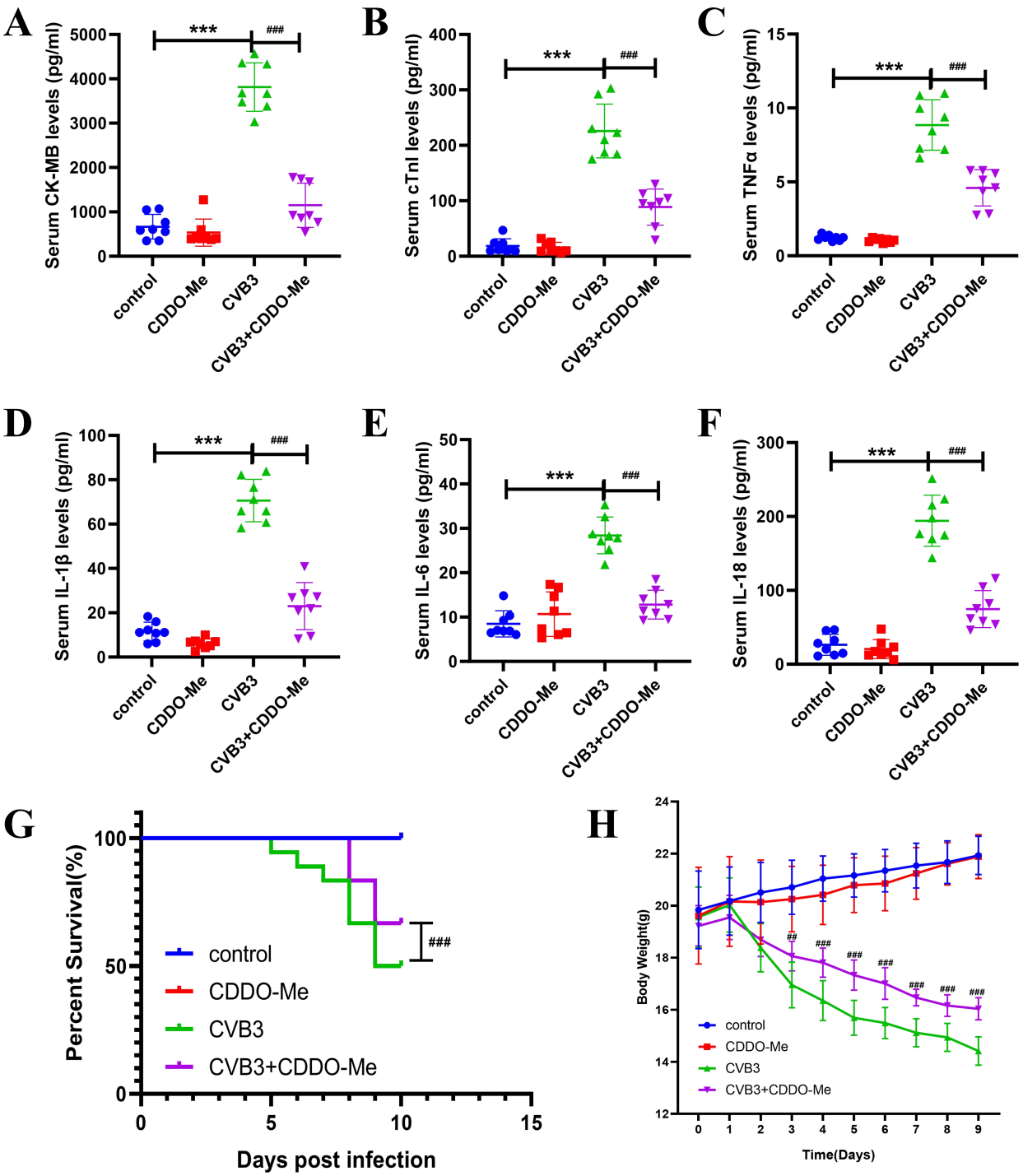

Fig. 1. CDDO-Me improved myocardial damage, inflammation, and survival in mice with viral myocarditis. (A,B) Serum CK-MB and cTnI contents determined by ELISA (n = 8). (C-F) TNF-α, IL-1β, IL-6 and IL-18 contents in serum examined by ELISA (n = 8). (G) Survival curves for mice 10 days following CDDO-Me injection (n = 18). (H) Body weight alteration (n = 9). The results indicate means $\pm$ SD. *** $p < 0.001$ vs. control group; $^{\#\#}$ $p < 0.01$, $^{\#\#\#}$ $p < 0.001$ vs. CVB3 group. CDDO-Me, 2-cyano-3,12-dioxoolean-1,9-dien-28-oic acid; CK-MB, creatine kinase isoenzyme; cTnI, cardiac isoform of troponin I; ELISA, enzyme-linked immunosorbent assay; TNF-α, tumor necrosis factor-alpha; IL-, interleukin-; SD, standard deviations; CVB3, coxsackievirus B3.

CDDO-Me Ameliorates Inflammatory Response Among VMC Mice via the Nrf2/HO-1 Pathway

As mentioned earlier, Nrf2 serves as an important anti-inflammatory substance *in vivo*. Activated Nrf2 enters the nucleus and can stimulate the synthesis of downstream anti-inflammatory substances such as NQO-1 and HO-1 [17], thus playing an anti-inflammatory role. Phosphorylation, as a crucial change in the Nrf2 activation pathway, also

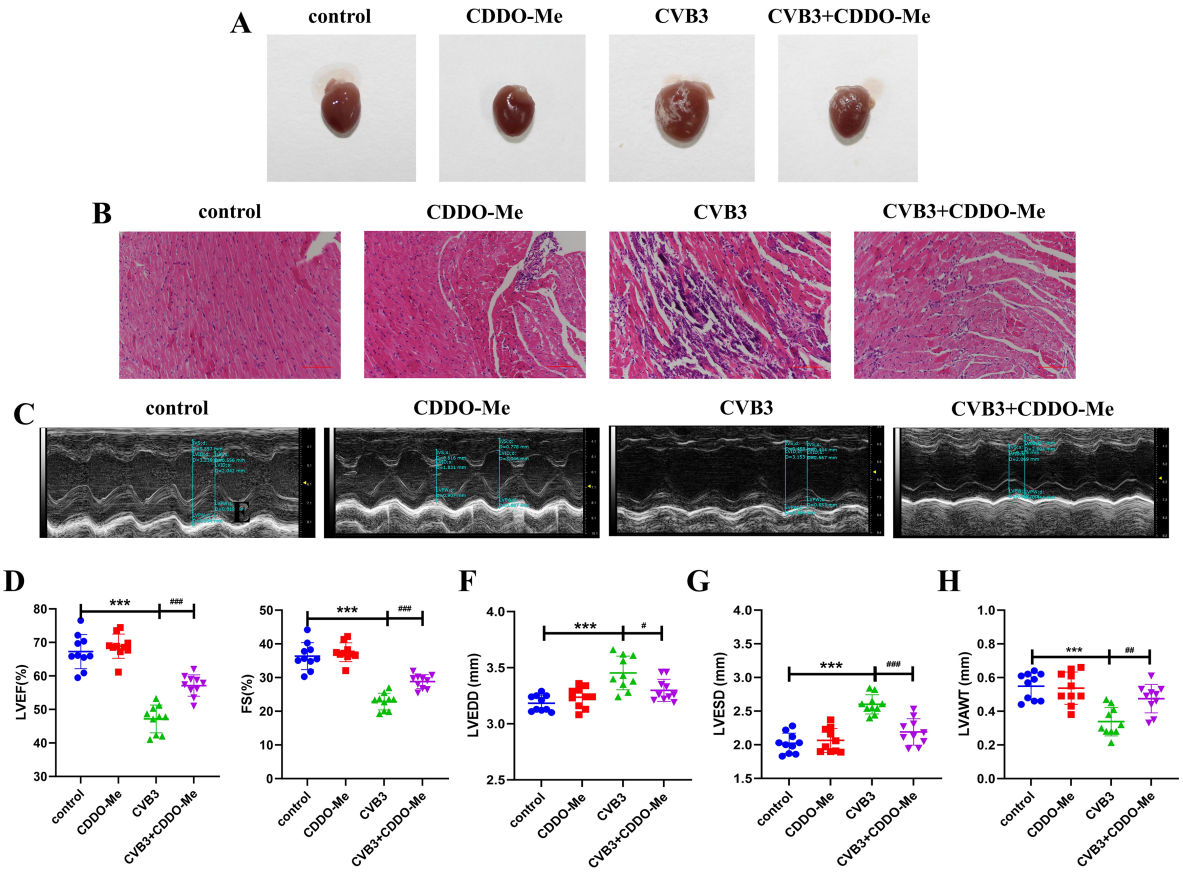

Fig. 2. CDDO-Me inhibited myocardial remodeling. (A) Representative images of the hearts of the mice (n = 6). (B) Typical micrographs showing H&E staining are shown for each group (n = 6, scale bar 100 μm). (C) Typical M-mode echocardiography image showing mouse left ventricular alterations (n = 10). (D–H) left ventricular ejection fraction (LVEF), fraction shortening (FS), left ventricular end-diastolic dimension (LVEDD), Left ventricular end-systolic dimension (LVESD), left ventricular anterior wall thickness (LVAWT) of the mice (n = 10). The values represent the means ± SD. *** $p < 0.001$ vs. control group; $^{\#}$ $p < 0.05$, $^{\#\#}$ $p < 0.01$, $^{\#\#\#}$ $p < 0.001$ vs. CVB3 group. H&E, hematoxylin-eosin.

contributes to the subsequent anti-inflammatory regulation [18]. In our research, according to the immunofluorescence results, p-Nrf2, HO-1, and NQO-1 levels within the mouse myocardium decreased following CVB3 infection ($p < 0.001$ or $p < 0.01$). However, their expression were significantly increased to varying degrees after CDDO-Me treatment ($p < 0.001$ or $p < 0.01$) (Fig. 4A,B). As shown in Fig. 4C,D, we determined the protein levels in the mouse myocardium by a WB assay. These protein contents decreased within the mouse myocardium after CVB3 infection relative to the control group ($p < 0.001$), whereas they were significantly improved after CDDO-Me intervention ($p < 0.001$, $p < 0.01$ or $p < 0.05$). The levels of these mRNAs within the mouse myocardium were subsequently determined through qRT-PCR (Fig. 4E). From the above findings, these mRNA levels in the mouse myocardium decreased after CVB3 infection; however, the changes were reversed following CDDO-Me treatment.

CDDO-Me Improved H9C2 Cell Survival After CVB3 Co-Incubation

For exploring CDDO-Me's biological safety, H9C2 cells underwent CDDO-Me treatment at varying doses (0, 0.01, 0.05, 0.1, 0.5, or 1 μM) for 12, 24 or 48 h, separately. Thereafter, we used the CCK-8 assay to measure cell viability. As shown in Fig. 5A,B, H9C2 cell viability was 88.4%, 92.83% and 82.31%, respectively, after 12, 24, and 48 h of coincubation with 0.1 μM CDDO-Me. Therefore, we incubated H9C2 cells using 0.1 μM CDDO-Me for a 24 h duration for subsequent *in vitro* studies. We randomized H9C2 cells into control, CDDO-Me, CVB3, and CVB3+CDDO-Me groups and added 0.6 ml of 100 $TCID_{50}$ ($TCID_{50}$ = 7.4, analyzed by the Reed–Muench approach) virus to the CVB3 and the CVB3+CDDO-Me groups, whereas DMSO at an identical amount was introduced in both the CDDO-Me and the control groups [14,18]. After 2 h of infection, H9C2 cells in the CDDO-ME and the CVB3+CDDO-Me

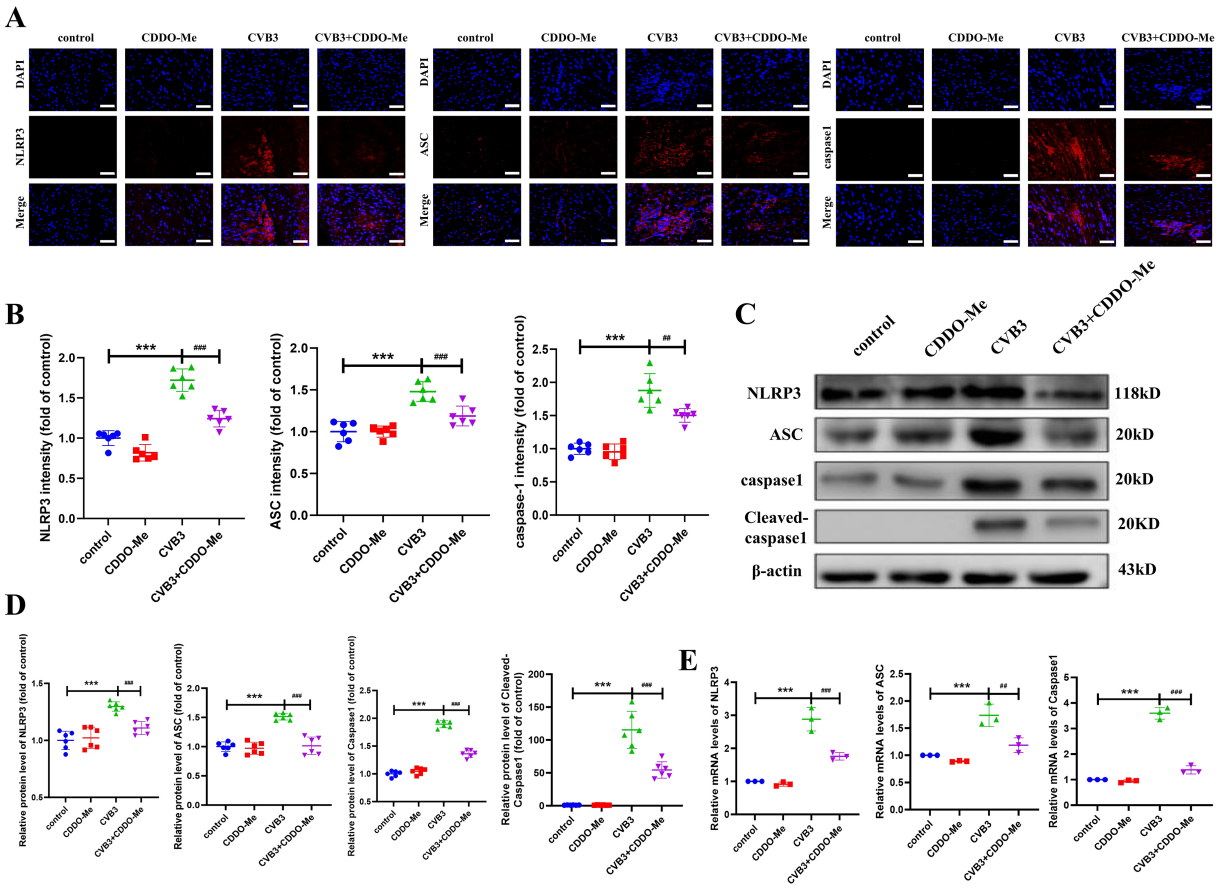

Fig. 3. CDDO-Me decreases NLRP3 inflammasome activation within the mouse heart. (A) Typical immunofluorescence images for NLRP3, ASC, and Caspase-1 within cardiac tissue. Images from the top down show cell nuclei after staining with DAPI (blue), NLRP3, ASC, and Caspase-1 fluorescence (red), alongside merged images (n = 6, scale bar 50 μm). (B) Quantitative analysis of NLRP3, ASC, and Caspase-1 within cardiac tissue (n = 6). (C,D) Western blots and NLRP3, ASC, and Caspase-1 and cleaved Caspase-1 protein levels inside cardiac tissue (n = 6). (E) NLRP3, ASC, and Caspase-1 mRNA levels within cardiac tissue from every group were determined via qRT-PCR (n = 6). Values represent the means ± SD. *** $p < 0.001$ vs. control group, $^{\#\#}$ $p < 0.01$, $^{\#\#\#}$ $p < 0.001$ vs. CVB3 group. NLRP3, nucleotide oligomerization domain-, leucine-rich repeat-, and pyrin domain-containing protein 3; ASC, apoptotic-associated speck-like protein containing a CARD.

groups were co-incubated with 0.1 μM CDDO-Me for a 24-h duration, subsequently, a CCK-8 assay was implemented to evaluate the H9C2 cell viability. H9C2 cell viability after co-incubation with CVB3 was significantly reduced ($p < 0.001$), and CDDO-Me intervention partially reversed the CVB3-induced reduction in H9C2 cell viability ($p < 0.01$) (Fig. 5C). In addition, we determined inflammatory factor contents, such as TNF-α, IL-1β, IL-6 and IL-18, within the H9C2 cell supernatants from each treatment group by ELISA, and the results are shown in Fig. 5D. These inflammatory factor contents in the CVB3 group apparently increased ($p < 0.001$), however, their levels markedly decreased in the CDOO-Me-treated group ($p < 0.001$ or $p < 0.01$). These results showed that CDOO-Me treatment significantly reduces the level of CVB3-induced H9C2 injury and inflammation.

CDDO-Me Inhibits NLRP3 Inflammasome Activation Within CVB3-Treated H9C2 Cells

Immunofluorescence experiments were carried out to analyze the inflammasome activation-related protein contents, including ASC, Caspase-1 and NLRP3, for exploring the inflammatory responses induced by CVB3 inside H9C2 cells. Notably, H9C2 cell grouping and treatment were conducted as previously described. Our findings revealed that ASC, Caspase-1 and NLRP3 protein levels were markedly elevated in H9C2 cells co-incubated with CVB3 ($p < 0.001$), and CDDO-Me treatment significantly attenuated the upregulation of the ASC, Caspase-1 and NLRP3 proteins in CVB3-induced H9C2 cells ($p < 0.001$ or $p < 0.01$) (Fig. 6A,B). We further explored inflammasome activation-associated mRNA and protein levels through qRT-PCR and WB, separately. The WB experiments showed that the ASC, Caspase-1, cleaved Caspase-1

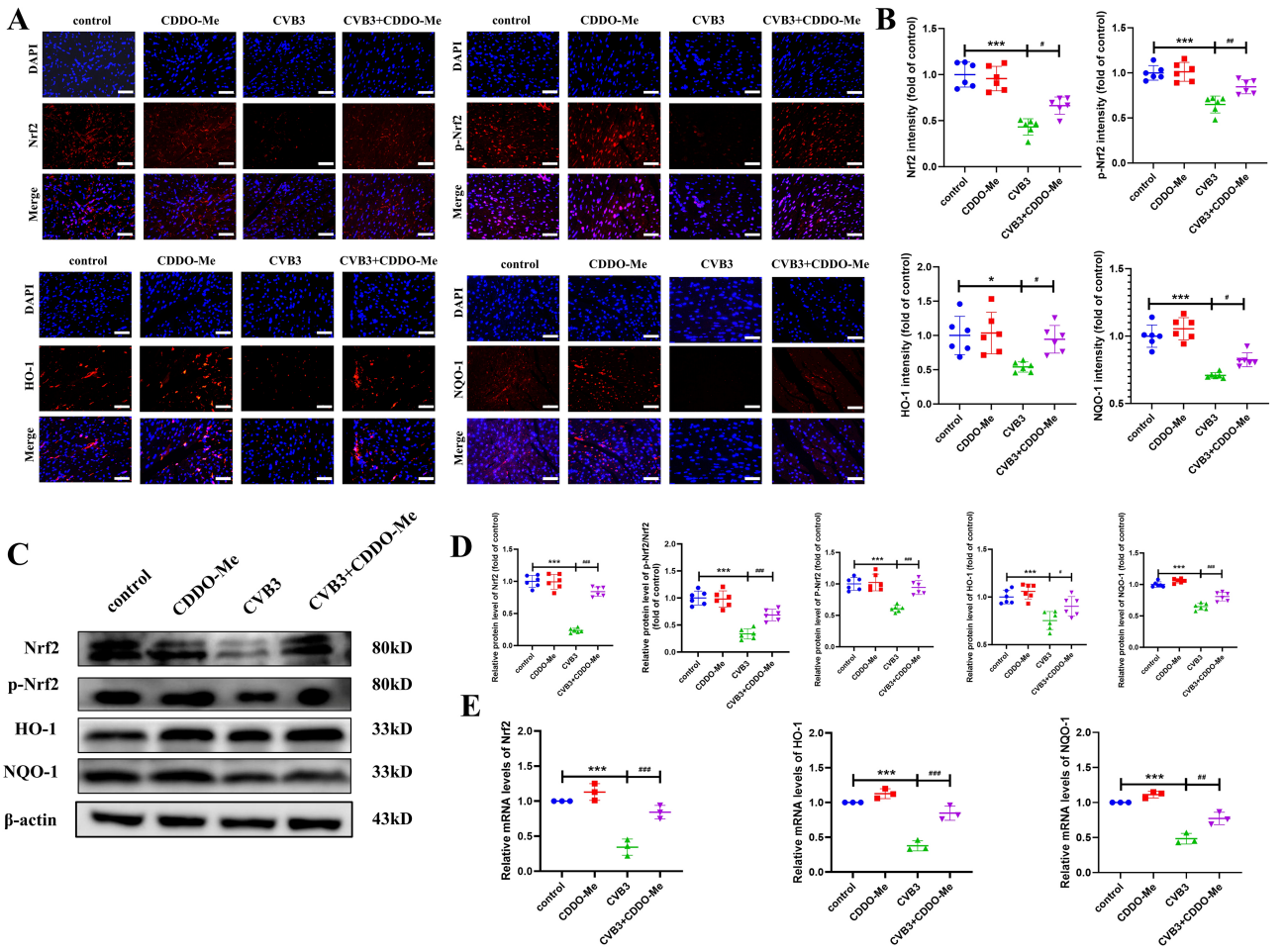

Fig. 4. CDDO-Me ameliorates the inflammatory response in VMC mice via the Nrf2/HO-1 pathway. (A) Typical immunofluorescence images for Nrf2, P-Nrf2, HO-1, and NQO-1 in cardiac tissue. Images from the top down indicate cell nuclei after staining with DAPI (blue); Nrf2, P-Nrf2, HO-1, and NQO-1 fluorescence (red) as well as merged images (n = 6, scale bar 50 μm). (B) Quantification of the proteins above inside cardiac tissue (n = 6). (C,D) Western blots and the levels of the protein above within cardiac tissue (n = 6). (E) The levels of the genes above within cardiac tissue were measured through qRT-PCR from each group (n = 6). The values represent the means ± SD. * $p < 0.05$, *** $p < 0.001$ vs. control group; $^{\#}$ $p < 0.05$, $^{\#\#}$ $p < 0.01$, $^{\#\#\#}$ $p < 0.001$ vs. CVB3 group. VMC, viral myocarditis; Nrf2, Nuclear factor erythroid 2-related factor 2; HO-1, heme oxygenase-1; NQO-1, NAD(P)H quinone oxidoreductase 1.

and NLRP3 protein levels were markedly elevated within H9C2 cells co-incubated with CVB3 ($p < 0.001$) and that the upregulation of these inflammasome activation-related proteins was inhibited by CDDO-Me treatment ($p < 0.001$ or $p < 0.05$) (Fig. 6C,D). qRT-PCR revealed that ASC, caspase-1, and NLRP3 mRNA expression in H9C2 cells co-incubated with CVB3 was significantly greater than that in H9C2 cells ($p < 0.001$), however, the expression of these inflammasome activation-related mRNAs was reduced to varying degrees after CDDO-Me treatment ($p < 0.001$ or $p < 0.01$) (Fig. 6E). These results showed that CDDO-Me inhibited NLRP3 inflammasome activation within CVB3-treated H9C2 cells.

CDDO-Me Activates Nrf2/HO-1 Pathway Within the CVB3-Treated H9C2 Cells

In vitro, this study further verified how Nrf2/HO-1 pathway affects CVB3-induced inflammatory response in viral myocarditis. As expected, immunofluorescence analysis suggested that Nrf2, P-Nrf2, HO-1, and NQO-1 protein contents markedly decreased inside CVB3-treated H9C2 cells ($p < 0.001$), and the downregulation of these proteins was effectively alleviated by CDDO-Me treatment ($p < 0.01$ or $p < 0.05$) (Fig. 7A,B). Furthermore, as shown in Fig. 7C,D, following the WB assay, the protein contents of these H9C2 cells were markedly lower than those of the control H9C2 cells after CVB3 treatment ($p < 0.001$), while the downregulation of these proteins was improved by CDDO-Me intervention ($p < 0.001$ or $p < 0.01$). Additionally, qRT-PCR revealed that the mRNA levels in the

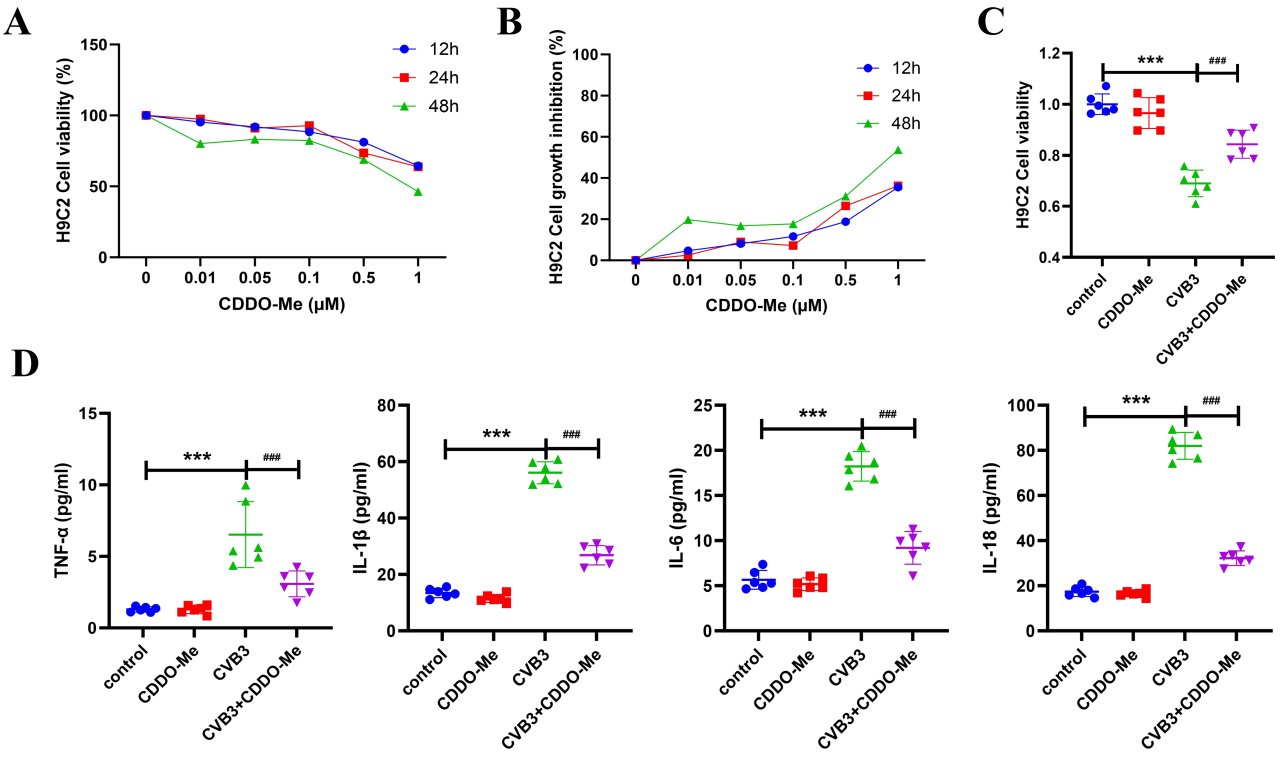

Fig. 5. CDDO-Me improves the survival of H9C2 cells co-incubated with CVB3. (A,B) CCK-8 assay was conducted for assessing cell viability and cell growth inhibition after exposure to various concentrations of CDDO-Me (n = 6). (C) H9C2 cell viability in diverse treatment groups was evaluated through the CCK-8 assay (n = 6). (D) ELISA was conducted for determining the TNF-α, IL-1β, IL-6 and IL-18 contents inside H9C2 cell supernatants of each treatment group (n = 6). Results indicate means ± SD. *** $p < 0.001$ vs. control group; $^{\#\#\#}$ $p < 0.001$ vs. CVB3 group. CCK-8, Cell Counting Kit-8.

CVB3-treated H9C2 cells were significantly decreased ($p < 0.001$), however, these changes were reversed in H9C2 cells treated with CDDO-Me ($p < 0.001$ or $p < 0.01$) (Fig. 7E). These results suggest that CDDO-Me may mitigate CVB3-induced H9C2 cardiomyocyte damage by regulating the Nrf2/HO-1 signaling axis.

Inhibiting Nrf2/HO-1 Pathway Aggravates CVB3-Induced NLRP3 Inflammasome Activation Within H9C2 Cells

To determine the relationship between the Nrf2/HO-1 pathway and the CVB3-mediated NLRP3 inflammasome activation, we treated H9C2 cells with Nrf2-specific small interfering RNA (si-Nrf2) for a 24h duration to suppress Nrf2 expression, and also treated some H9C2 cells using si-NC for the same duration. Then, H9C2 cells were randomly divided into 7 groups: control, si-NC, si-Nrf2, si-NC+CVB3, si-Nrf2+CVB3, si-NC+CVB3+CDDO-Me and si-Nrf2+CVB3+CDDO-Me. Among these, cells in the si-NC+CVB3 and si-Nrf2+CVB3 groups were treated with 100 $TCID_{50}$ virus for 2 h. Following the same viral treatment, cells in the si-NC+CVB3+CDDO-Me and si-Nrf2+CVB3+CDDO-Me groups were further incubated with 0.1 μM CDDO-Me for an additional 24 h. As shown in Fig. 8A, CCK-8 experiments revealed the significantly reduced H9C2 cell viability after incubation with CVB3, and Nrf2 knockdown also significantly inhibited H9C2 cell viability. Moreover, after Nrf2 knockdown and co-incubation with CVB3, H9C2 cell viability was also decreased, although these observed changes were reversed by CDDO-Me intervention. Additionally, as presented in Fig. 8B,C, WB analysis revealed markedly decreased Nrf2 levels in H9C2 cells after si-Nrf2 treatment ($p < 0.001$), indicating that we successfully constructed an Nrf2-knockdown cell model. Similarly, HO-1 and NQO-1 downstream regulators of Nrf2, also had significantly reduced levels, and the phosphorylation level of Nrf2 was also attenuated ($p < 0.001$). Notably, Nrf2, P-Nrf2, HO-1, and NQO-1 protein contents were lower within H9C2 cells after Nrf2 knockdown and co-incubation with CVB3 than in those after si-Nrf2 treatment. These changes were reversed by the CDDO-Me intervention. Moreover, our experiments revealed that Nrf2 knockdown significantly triggered inflammation inside H9C2 cells, as suggested by the increased expression of inflammasome activation-related proteins, such as ASC, Caspase-1, cleaved Caspase-1 and NLRP3 ($p < 0.001$ or $p < 0.05$). Correspondingly, ASC, Caspase-1, and NLRP3 protein levels were elevated within H9C2 cells after Nrf2 knockdown and co-incubation with CVB3 than in those after si-Nrf2 treatment. These changes were reversed

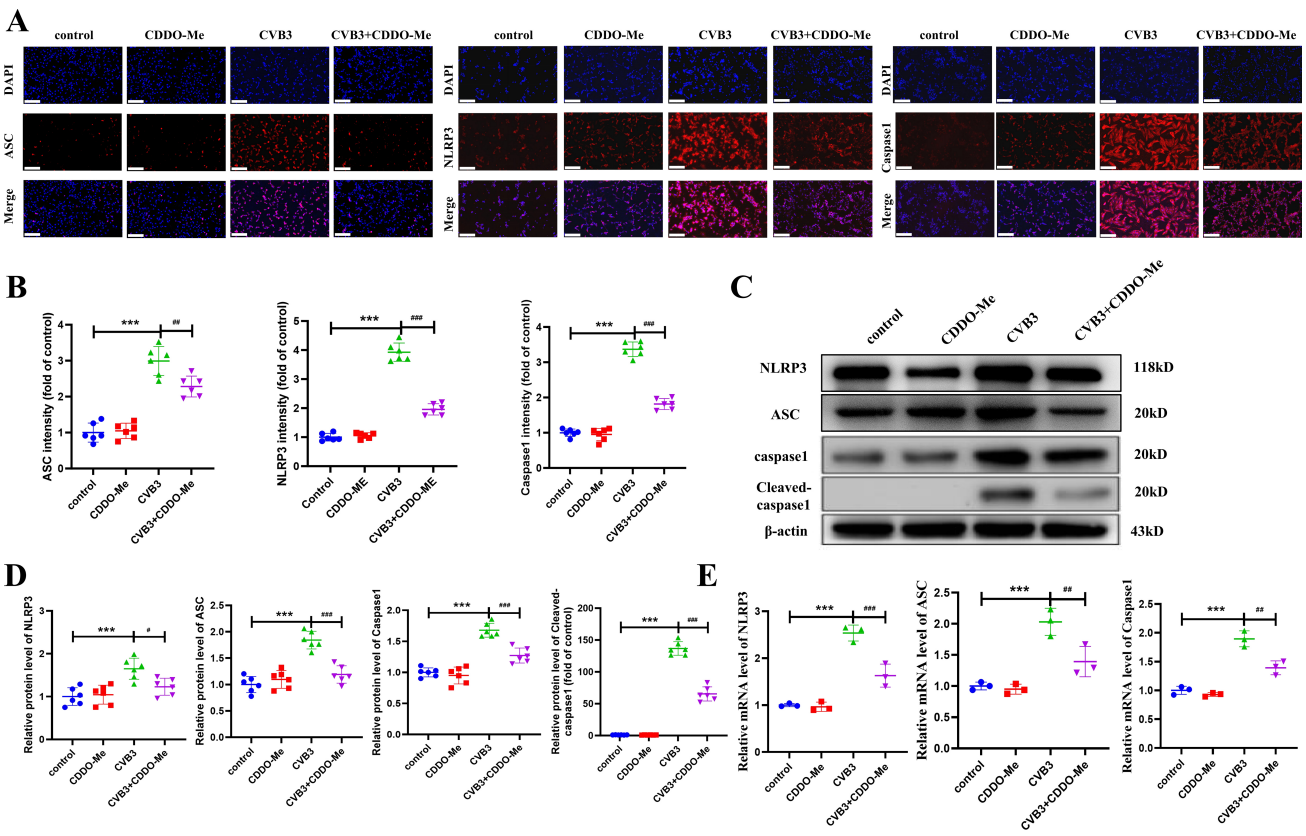

Fig. 6. CDDO-Me inhibits NLRP3 inflammasome activation in CVB3-treated H9C2 cells. (A) Typical immunofluorescence images for ASC, NLRP3, and Caspase-1 in H9C2 cells. The images from top to bottom display the cell nuclei after staining with DAPI (blue), ASC, NLRP3, and Caspase-1 fluorescence (green), as well as merged images (n = 6, scale bar 200 μm). (B) Quantification of ASC, NLRP3, and Caspase-1 within H9C2 cells (n = 6). (C,D) Western blots and NLRP3, ASC, and Caspase-1 and Cleaved Caspase-1 levels inside H9C2 cells (n = 6). (E) NLRP3, ASC, and Caspase-1 mRNA expression inside H9C2 cells was analyzed through qRT-PCR for each group (n = 6). The values represent the means ± SD. *** $p < 0.001$ vs. control group; $^{\#}$ $p < 0.05$, $^{\#\#}$ $p < 0.01$, $^{\#\#\#}$ $p < 0.001$ vs. CVB3 group.

by CDDO-Me intervention (Fig. 8D,E). The above results indicate that CDDO-Me can significantly improve CVB3-induced inflammasome activation in H9C2 cells, probably through modulating the Nrf2/HO-1 pathway.

Discussion

Viral myocarditis can induce myocardial structural changes, cardiac dysfunction, various arrhythmias, and even cardiac arrest [19,20]. At the tissue and cell levels, viral myocarditis progresses in 3 stages: the acute stage, where the virus enters into the host and replicates there, the subacute stage, in which the host's immune system is activated; and the chronic stage, in which cardiac remodeling occurs [21,22]. In the acute stage, many viruses enter into the cardiomyocytes, viral replication causes acute myocyte injury, further leading to cardiomyocyte necrosis, apoptosis, intracellular antigen exposure, etc., and ultimately activating the host immune system. The subacute phase usually lasts for several weeks to months and is characterized mainly by activated virus-specific T lymphocytes probably targeting host organs through molecular mimicry. During this process, cardiac damage and contractile dysfunction are caused mainly by reactive processes such as cytokine activation (TNFα, IL-1, IL-6) as well as antibodies to viruses and cardiac proteins [23–25]. In many myocarditis patients, the immune response decreases after the virus is eliminated, and the left ventricular function recovers with no sequelae. Nonetheless, in certain mouse models or humans, (auto)immune processes persist regardless of whether the virus genome is detected within the myocardium, resulting in the chronic stage characterized by myocardial remodeling and DCM occurrence [21,26,27]. In this study, we verified that myocardial injury and left ventricular systolic dysfunction are characteristic features of CVB3-induced viral myocarditis, manifested by elevated CK-MB and cTnI levels in the serum (myocardial injury markers), and that the LVEF and FS markedly decreased while the systolic diameter apparently increased.

In myocarditis, initial immune activation can limit viral spread and is thereby good for the host, nonetheless, regardless of whether the immune response persists or is

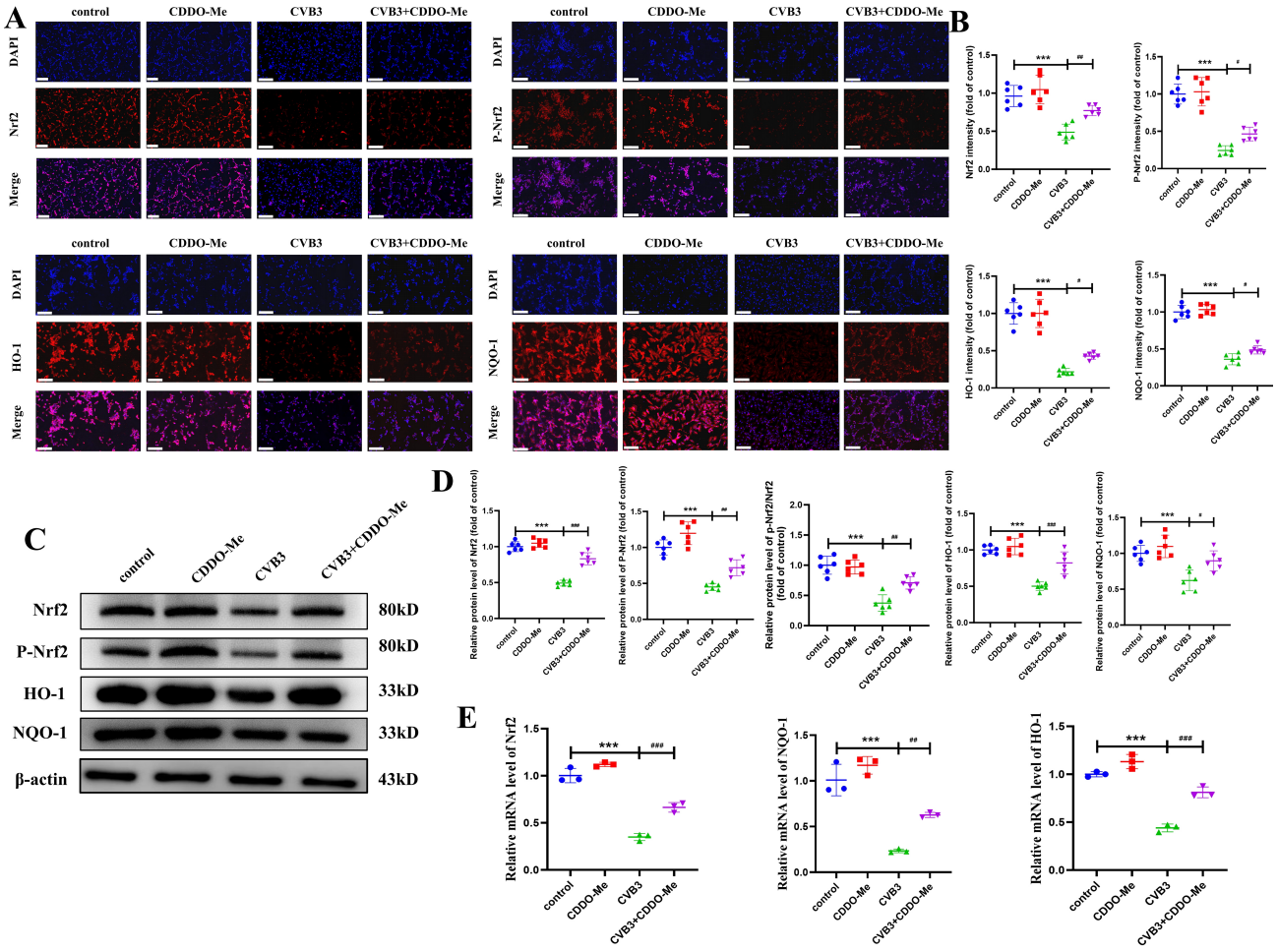

Fig. 7. CDDO-Me ameliorates the inflammatory response in H9C2 cells treated with CVB3 via Nrf2/HO-1 pathway. (A) Representative immunofluorescence images showing Nrf2, P-Nrf2, HO-1, and NQO-1 inside H9C2 cells. The images from the top down show cell nuclei after staining with DAPI (blue); Nrf2, P-Nrf2, HO-1, and NQO-1 fluorescence (red) as well as merged images of both proteins (n = 6, scale bar 200 μm). (B) Quantification for these above proteins within H9C2 cells (n = 6). (C,D) Western blots and the above protein contents within H9C2 cells (n = 6). (E) These above gene expression inside H9C2 cells was measured through qRT-PCR for each group (n = 6). The values represent the means ± SD. *** $p < 0.001$ vs. control group; $^{\#}$ $p < 0.05$, $^{\#\#}$ $p < 0.01$, $^{\#\#\#}$ $p < 0.001$ vs. CVB3 group.

too strong, it can induce unfavorable outcomes, promoting myocarditis and DCM occurrence. Therefore, immune response modulation can assist in mitigating the harmful effects induced by the host immune response and suppress myocarditis progression [28–30]. NLRP3 is the crucial innate immune system sensor capable of detecting endogenous cell injury and exogenous pathogen invasion and responding through the generation of NLRP3 inflammasome, the supramolecular complex activating caspase-1 [31,32]. The NLRP3 inflammasome comprises NLRP3 (responsible for capturing danger signals while recruiting downstream molecules), caspase-1 (capable of eliciting the maturation of cytokines such as IL-1β and IL-18 alongside gasdermin D processing to mediate mediator secretion and pyroptosis), and ASC (bridging NLRP3 with caspase-1) [33–35]. Numerous studies have demonstrated that overactivation of the NLRP3 inflammasome induces the release of various inflammatory factors in tissue cells—including pro-inflammatory cytokines such as TNF-α, IL-1β, IL-6, and IL-18—through synergistic regulatory mechanisms [31,36]. According to our results, NLRP3, caspase-1, and ASC levels were markedly elevated in cardiomyocytes with CVB3-induced viral myocarditis, and notably, inflammation-related indicators such as TNF-α, IL-1β, IL-6 and IL-18 showed markedly elevated levels.

Nrf2 regulates cellular defenses to resist oxidative or toxic stresses via regulating oxidative stress response- and drug detoxification-related gene levels [37,38]. After Nrf2 is activated, cells can become resistant to inflammatory stresses and chemical carcinogens. Apart from its antioxidant capacity, Nrf2 participates in numerous cell events, such as inflammation and metabolism, and exerts a wider

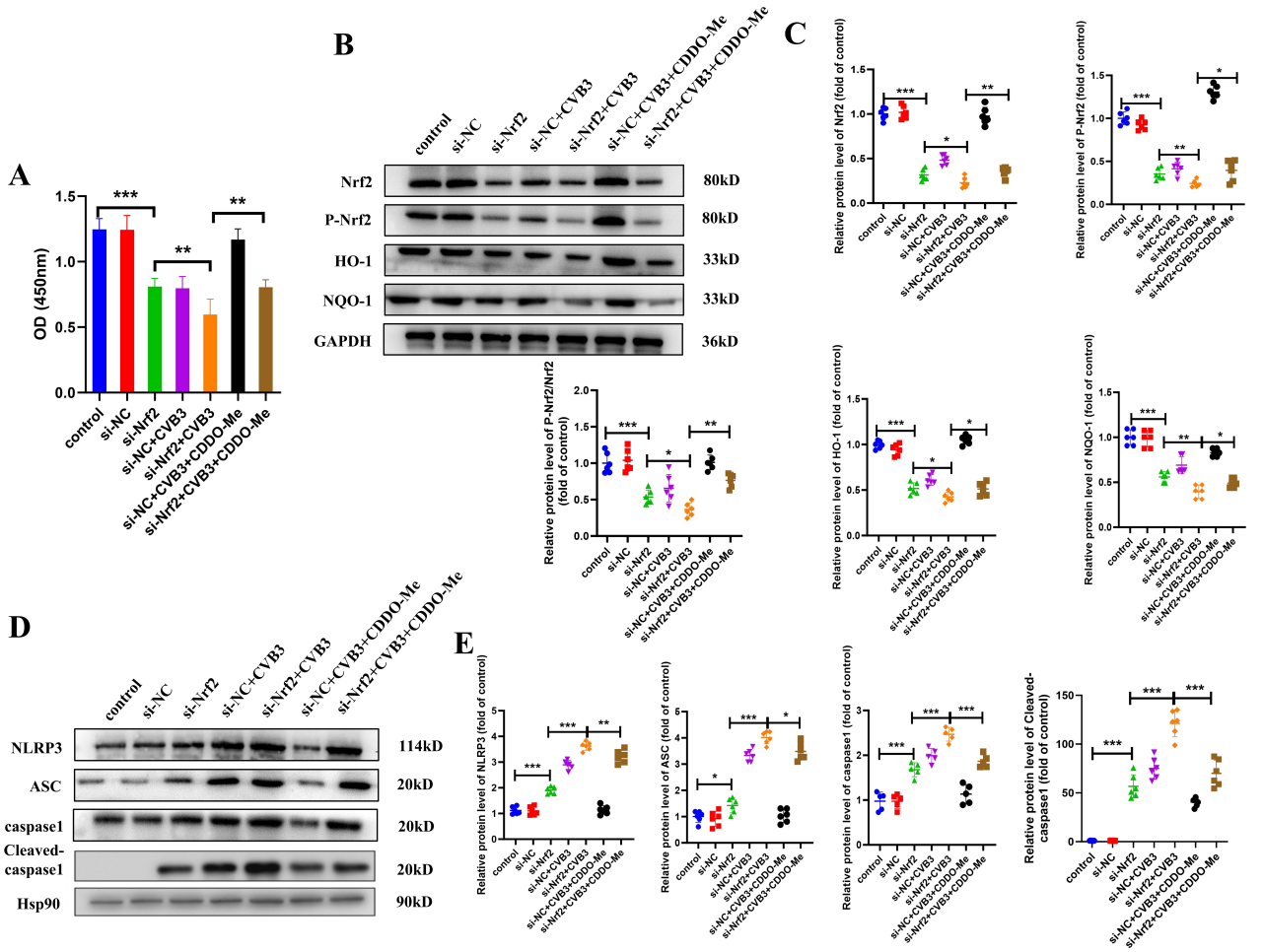

Fig. 8. Inhibiting Nrf2/HO-1 pathway aggravates the inflammatory response induced by CVB3 within H9C2 cells. (A) The H9C2 cell viability in every treatment group was measured through CCK-8 method (n = 6). (B,C) Western blots showing Nrf2, P-Nrf2, HO-1 and NQO-1 protein levels inside H9C2 cells (n = 6). (D,E) Western blots demonstrating NLRP3, ASC, caspase-1 and cleaved caspase-1 protein levels in H9C2 cells (n = 6). Results indicate means ± SD. * $p < 0.05$, ** $p < 0.01$, *** $p < 0.001$.

range of effects than initially anticipated [39–41]. HO-1 can catalyze a rate-limiting step during heme oxidative degradation; in addition, it can be quickly transformed into bilirubin and exerts a key effect on regulating inflammation, oxidative stress, and apoptosis [42]. Like other antioxidant proteins, Nrf2 immediately regulates HMOX1 expression, a gene encoding HO-1. Therefore, Nrf2 has been suggested to regulate HO-1 expression *in vivo* and *in vitro* to resist inflammation [43–45]. In this work, Nrf2 expression and phosphorylation markedly decreased during CVB3-mediated virus myocarditis, and the corresponding downstream protein levels (NQO-1 and HO-1) significantly decreased; however, these changes were attenuated following CDDO-ME administration.

Moreover, triterpenoids are utilized as medicines across numerous Asian countries because of their effects on proliferation, inflammation, oxidation, carcinogenesis, and tumors [46–48]. CDDO-Me is a derivative of synthetic triterpenoids, which are endogenous activators of Nrf2 that are closely associated with inflammation relief and suppression of NF-κB activity [13]. As demonstrated by Rajesh K Thimmulappa *et al.* [49], triterpenoids (CDDO-Im, CDDO-Me) target Nrf2 pathway, thereby protecting against LPS-mediated reactive oxygen species and inflammatory responses within human neutrophils/peripheral blood mononuclear cells because triterpenoids promote Nrf2 protein nuclear translocation. These findings indicate that LPS-mediated inflammatory responses can be prevented through activating Nrf2-mediated antioxidative pathway via CDDO-Im or CDDO-Met [49]. In addition, Fakhar H Waqas *et al.* [50] reported that NRF2 activators interfere with the nucleocytoplasmic export of viral RNPs independent of NRF2 to suppress influenza A virus replication, indicating that, in addition to exerting anti-inflammatory and antioxidative effects, cytoprotective Nrf2 pathway activators can resist viral infection. In this study, we verified that CDDO-Me, a derivative of synthetic triterpenoids, can significantly induce the phosphorylation of

Nrf2 in cardiomyocytes in CVB3-induced viral myocarditis, thus exerting an anti-inflammatory effect and improving the myocardial injury and myocardial remodeling induced by viral myocarditis.

Our study has several limitations that should be acknowledged. First, the findings are primarily derived from experiments conducted in a murine model of viral myocarditis and in H9C2 cardiomyocytes, they cannot fully recapitulate the complexity of human disease. Second, this study focused on the protective efficacy and mechanism of CDDO-Me, and did not systematically evaluate its potential adverse effects or optimal dosing window *in vivo*. Future studies should therefore include detailed toxicological assessments and dose-response evaluations to better define its therapeutic window. Despite these limitations, our study provides several novel insights. This is the first report demonstrating that CDDO-Me, a potent synthetic triterpenoid and Nrf2 activator, can alleviate CVB3-induced myocardial injury by simultaneously mitigating oxidative stress and inflammation. Mechanistically, we delineated that this protection is largely mediated through the activation of the Nrf2/HO-1 signaling axis, providing a clear molecular basis for its action. CDDO-Me with its dual antioxidant and anti-inflammatory properties acting through a well-defined pathway (Nrf2), represents a promising targeted therapeutic approach.

Conclusions

According to our findings, CDDO-ME antagonizes CVB3-mediated myocardial injury and NLRP3 inflammasome-mediated inflammatory responses, which is achieved by activating Nrf2 while upregulating the downstream proteins HO-1 and NQO1 in viral myocarditis. These findings lay a potential theoretical foundation and experimental direction for developing targeted therapies for CVB3-induced viral myocarditis.

Availability of Data and Materials

All datasets utilized in this work are available from the corresponding author on request.

Author Contributions

CM designed the research study and made the first draft; XRC, XNS, RFZ, PCY performed the research; CM and XNS collected and analyzed the data. All authors have been involved in revising it critically for important intellectual content. All authors gave final approval of the version to be published. All authors have participated sufficiently in the work to take public responsibility for appropriate portions of the content and agreed to be accountable for all aspects of the work in ensuring that questions related to its accuracy or integrity.

Ethics Approval and Consent to Participate

All animal experiments were approved by the Ethics Committee of Shandong Medical University (NO: 2022–302).

Acknowledgment

Not applicable.

Funding

This research received no external funding.

Conflict of Interest

The authors declare no conflict of interest.

Supplementary Material

Supplementary material associated with this article can be found, in the online version, at https://doi.org/10.24976/Discov.Med.202638206.75.

References

[1] Sagar S, Liu PP, Cooper LT, Jr. Myocarditis. Lancet. 2012; 379: 738–747. https://doi.org/10.1016/S0140-6736(11)60648-X.

[2] Rose NR. Viral myocarditis. Current Opinion in Rheumatology. 2016; 28: 383–389. https://doi.org/10.1097/BOR.0000000000000303.

[3] Pollack A, Kontorovich AR, Fuster V, Dec GW. Viral myocarditis–diagnosis, treatment options, and current controversies. Nature Reviews. Cardiology. 2015; 12: 670–680. https://doi.org/10.1038/nrcardio.2015.108.

[4] Zhang Y, Zhou X, Chen S, Sun X, Zhou C. Immune mechanisms of group B coxsackievirus induced viral myocarditis. Virulence. 2023; 14: 2180951. https://doi.org/10.1080/21505594.2023.2180951.

[5] Lasrado N, Reddy J. An overview of the immune mechanisms of viral myocarditis. Reviews in Medical Virology. 2020; 30: 1–14. https://doi.org/10.1002/rmv.2131.

[6] Kühl U, Schultheiss HP. Viral myocarditis: diagnosis, aetiology and management. Drugs. 2009; 69: 1287–1302. https://doi.org/10.2165/00003495-200969100-00001.

[7] Lei Z, Cao J, Wu J, Lu Y, Ni L, Hu X. Identification of the communal pathogenesis and immune landscape between viral myocarditis and dilated cardiomyopathy. ESC Heart Failure. 2024; 11: 282–292. https://doi.org/10.1002/ehf2.14585.

[8] Ahmed SMU, Luo L, Namani A, Wang XJ, Tang X. Nrf2 signaling pathway: Pivotal roles in inflammation. Biochimica et Biophysica Acta. Molecular Basis of Disease. 2017; 1863: 585–597. https://doi.org/10.1016/j.bbadis.2016.11.005.

[9] Garstkiewicz M, Strittmatter GE, Grossi S, Sand J, Fenini G, Werner S, *et al*. Opposing effects of Nrf2 and Nrf2-activating compounds on the NLRP3 inflammasome independent of Nrf2-mediated gene expression. European Journal of Immunology. 2017; 47: 806–817. https://doi.org/10.1002/eji.201646665.

[10] Zhang C, Zhao M, Wang B, Su Z, Guo B, Qin L, *et al*. The Nrf2-NLRP3-caspase-1 axis mediates the neuroprotective effects of Celastrol in Parkinson's disease. Redox Biology. 2021; 47: 102134. https://doi.org/10.1016/j.redox.2021.102134.

[11] Chen Z, Zhong H, Wei J, Lin S, Zong Z, Gong F, *et al*. Inhibition of Nrf2/HO-1 signaling leads to increased activation of the NLRP3 inflammasome in osteoarthritis. Arthritis Research & Therapy. 2019; 21: 300. https://doi.org/10.1186/s13075-019-2085-6.

[12] Toldo S, Abbate A. The role of the NLRP3 inflammasome and pyroptosis in cardiovascular diseases. Nature Reviews. Cardiology. 2024; 21: 219–237. https://doi.org/10.1038/s41569-023-00946-3.

[13] Wang YY, Yang YX, Zhe H, He ZX, Zhou SF. Bardoxolone methyl (CDDO-Me) as a therapeutic agent: an update on its pharmacokinetic and pharmacodynamic properties. Drug Design, Development and Therapy. 2014; 8: 2075–2088. https://doi.org/10.2147/DDDT.S68872.

[14] Sun Q, Ye F, Liang H, Liu H, Li C, Lu R, *et al*. Bardoxolone and bardoxolone methyl, two Nrf2 activators in clinical trials, inhibit SARS-CoV-2 replication and its 3C-like protease. Signal Transduction and Targeted Therapy. 2021; 6: 212. https://doi.org/10.1038/s41392-021-00628-x.

[15] Zhang Y, Zhu L, Li X, Ge C, Pei W, Zhang M, *et al*. M2 macrophage exosome-derived lncRNA AK083884 protects mice from CVB3-induced viral myocarditis through regulating PKM2/HIF-1α axis mediated metabolic reprogramming of macrophages. Redox Biology. 2024; 69: 103016. https://doi.org/10.1016/j.redox.2023.103016.

[16] Tian C, Gao L, Zhang A, Hackfort BT, Zucker IH. Therapeutic Effects of Nrf2 Activation by Bardoxolone Methyl in Chronic Heart Failure. The Journal of Pharmacology and Experimental Therapeutics. 2019; 371: 642–651. https://doi.org/10.1124/jpet.119.261792.

[17] Liu T, Tong J, Shao C, Qu J, Wang H, Shi Y, *et al*. MicroRNA-324-3p Plays A Protective Role Against Coxsackievirus B3-Induced Viral Myocarditis. Virologica Sinica. 2021; 36: 1585–1599. https://doi.org/10.1007/s12250-021-00441-4.

[18] Li X, Yang Z, Nie W, Jiang J, Li S, Li Z, *et al*. Exosomes derived from cardiac progenitor cells attenuate CVB3-induced apoptosis via abrogating the proliferation of CVB3 and modulating the mTOR signaling pathways. Cell Death & Disease. 2019; 10: 691. https://doi.org/10.1038/s41419-019-1910-9.

[19] Corsten MF, Schroen B, Heymans S. Inflammation in viral myocarditis: friend or foe? Trends in Molecular Medicine. 2012; 18: 426–437. https://doi.org/10.1016/j.molmed.2012.05.005.

[20] Rezkalla SH, Kloner RA. Viral myocarditis: 1917-2020: From the Influenza A to the COVID-19 pandemics. Trends in Cardiovascular Medicine. 2021; 31: 163–169. https://doi.org/10.1016/j.tcm.2020.12.007.

[21] Kindermann I, Barth C, Mahfoud F, Ukena C, Lenski M, Yilmaz A, *et al*. Update on myocarditis. Journal of the American College of Cardiology. 2012; 59: 779–792. https://doi.org/10.1016/j.jacc.2011.09.074.

[22] Esfandiarei M, McManus BM. Molecular biology and pathogenesis of viral myocarditis. Annual Review of Pathology. 2008; 3: 127–155. https://doi.org/10.1146/annurev.pathmechdis.3.121806.151534.

[23] Rose NR. Myocarditis: infection versus autoimmunity. Journal of Clinical Immunology. 2009; 29: 730–737. https://doi.org/10.1007/s10875-009-9339-z.

[24] Liu PP, Opavsky MA. Viral myocarditis: receptors that bridge the cardiovascular with the immune system? Circulation Research. 2000; 86: 253–254. https://doi.org/10.1161/01.res.86.3.253.

[25] Marchant DJ, McManus BM. Regulating viral myocarditis: allografted regulatory T cells decrease immune infiltration and viral load. Circulation. 2010; 121: 2609–2611. https://doi.org/10.1161/CIRCULATIONAHA.110.960054.

[26] Wang C, Luo H. Crosstalk Between Innate Immunity and Autophagy in Viral Myocarditis Leading to Dilated Cardiomyopathy. Reviews in Medical Virology. 2024; 34: e2586. https://doi.org/10.1002/rmv.2586.

[27] Tschöpe C, Ammirati E, Bozkurt B, Caforio ALP, Cooper LT, Felix SB, *et al*. Myocarditis and inflammatory cardiomyopathy: current evidence and future directions. Nature Reviews. Cardiology. 2021; 18: 169–193. https://doi.org/10.1038/s41569-020-00435-x.

[28] Schwimmbeck PL, Bigalke B, Schulze K, Pauschinger M, Kühl U, Schultheiss HP. The humoral immune response in viral heart disease: characterization and pathophysiological significance of antibodies. Medical Microbiology and Immunology. 2004; 193: 115–119. https://doi.org/10.1007/s00430-003-0217-7.

[29] Huang CH, Vallejo JG, Kollias G, Mann DL. Role of the innate immune system in acute viral myocarditis. Basic Research in Cardiology. 2009; 104: 228–237. https://doi.org/10.1007/s00395-008-0765-5.

[30] Zanatta A, Carturan E, Rizzo S, Basso C, Thiene G. Story telling of myocarditis. International Journal of Cardiology. 2019; 294: 61–64. https://doi.org/10.1016/j.ijcard.2019.07.046.

[31] Kelley N, Jeltema D, Duan Y, He Y. The NLRP3 Inflammasome: An Overview of Mechanisms of Activation and Regulation. International Journal of Molecular Sciences. 2019; 20: 3328. https://doi.org/10.3390/ijms20133328.

[32] Toldo S, Mezzaroma E, Buckley LF, Potere N, Di Nisio M, Biondi-Zoccai G, *et al*. Targeting the NLRP3 inflammasome in cardiovascular diseases. Pharmacology & Therapeutics. 2022; 236: 108053. https://doi.org/10.1016/j.pharmthera.2021.108053.

[33] Fu J, Wu H. Structural Mechanisms of NLRP3 Inflammasome Assembly and Activation. Annual Review of Immunology. 2023; 41: 301–316. https://doi.org/10.1146/annurev-immunol-081022-021207.

[34] Zhao C, Zhao W. NLRP3 Inflammasome-A Key Player in Antiviral Responses. Frontiers in Immunology. 2020; 11: 211. https://doi.org/10.3389/fimmu.2020.00211.

[35] Seoane PI, Lee B, Hoyle C, Yu S, Lopez-Castejon G, Lowe M, *et al*. The NLRP3-inflammasome as a sensor of organelle dysfunction. The Journal of Cell Biology. 2020; 219: e202006194. https://doi.org/10.1083/jcb.202006194.

[36] Swanson KV, Deng M, Ting JPY. The NLRP3 inflammasome: molecular activation and regulation to therapeutics. Nature Reviews. Immunology. 2019; 19: 477–489. https://doi.org/10.1038/s41577-019-0165-0.

[37] Tonelli C, Chio IIC, Tuveson DA. Transcriptional Regulation by Nrf2. Antioxidants & Redox Signaling. 2018; 29: 1727–1745. https://doi.org/10.1089/ars.2017.7342.

[38] Panda H, Wen H, Suzuki M, Yamamoto M. Multifaceted Roles of the KEAP1-NRF2 System in Cancer and Inflammatory Disease Milieu. Antioxidants. 2022; 11: 538. https://doi.org/10.3390/antiox11030538.

[39] He F, Ru X, Wen T. NRF2, a Transcription Factor for Stress Response and Beyond. International Journal of Molecular Sciences. 2020; 21: 4777. https://doi.org/10.3390/ijms21134777.

[40] Herengt A, Thyrsted J, Holm CK. NRF2 in Viral Infection. Antioxidants. 2021; 10: 1491. https://doi.org/10.3390/antiox10091491.

[41] Murakami S, Motohashi H. Roles of Nrf2 in cell proliferation and differentiation. Free Radical Biology & Medicine. 2015; 88: 168–178. https://doi.org/10.1016/j.freeradbiomed.2015.06.030.

[42] Ryter SW. Heme Oxgenase-1, a Cardinal Modulator of Regulated Cell Death and Inflammation. Cells. 2021; 10: 515. https://doi.org/10.3390/cells10030515.

[43] Saha S, Buttari B, Panieri E, Profumo E, Saso L. An Overview of Nrf2 Signaling Pathway and Its Role in Inflammation. Molecules. 2020; 25: 5474. https://doi.org/10.3390/molecule

s25225474.

[44] Kobayashi EH, Suzuki T, Funayama R, Nagashima T, Hayashi M, Sekine H, *et al*. Nrf2 suppresses macrophage inflammatory response by blocking proinflammatory cytokine transcription. Nature Communications. 2016; 7: 11624. https://doi.org/10.1038/ncomms11624.

[45] Li W, Khor TO, Xu C, Shen G, Jeong WS, Yu S, *et al*. Activation of Nrf2-antioxidant signaling attenuates NFkappaB-inflammatory response and elicits apoptosis. Biochemical Pharmacology. 2008; 76: 1485–1489. https://doi.org/10.1016/j.bcp.2008.07.017.

[46] Özdemir Z, Wimmer Z. Selected plant triterpenoids and their amide derivatives in cancer treatment: A review. Phytochemistry. 2022; 203: 113340. https://doi.org/10.1016/j.phytochem.2022.113340.

[47] Zhao ZZ, Ji BY, Wang ZZ, Si YY, Sun YJ, Chen H, *et al*. Lanostane triterpenoids with anti-proliferative and anti-inflammatory activities from medicinal mushroom Ganoderma lingzhi. Phytochemistry. 2023; 213: 113791. https://doi.org/10.1016/j.phytochem.2023.113791.

[48] Gu C, Wang YQ, Su BJ, Hu YJ, Liao HB, Liang D. Triterpenoids and triterpenoid saponins from Vitex negundo and their anti-inflammatory activities. Phytochemistry. 2024; 222: 114068. https://doi.org/10.1016/j.phytochem.2024.114068.

[49] Thimmulappa RK, Fuchs RJ, Malhotra D, Scollick C, Traore K, Bream JH, *et al*. Preclinical evaluation of targeting the Nrf2 pathway by triterpenoids (CDDO-Im and CDDO-Me) for protection from LPS-induced inflammatory response and reactive oxygen species in human peripheral blood mononuclear cells and neutrophils. Antioxidants & Redox Signaling. 2007; 9: 1963–1970. https://doi.org/10.1089/ars.2007.1745.

[50] Waqas FH, Shehata M, Elgaher WAM, Lacour A, Kurmasheva N, Begnini F, *et al*. NRF2 activators inhibit influenza A virus replication by interfering with nucleo-cytoplasmic export of viral RNPs in an NRF2-independent manner. PLoS Pathogens. 2023; 19: e1011506. https://doi.org/10.1371/journal.ppat.1011506.